ON THE BOGIE HUNTING IN A TRACK WITH RANDOM IRREGULATIRIES

MĂDĂLINA DUMITRIU[1]

Abstract: Hunting movement of a railway vehicle is a consequence of the reversed conic shape of the rolling surfaces. When the speed is higher than a particular value – the critical speed – the hunting movement has the feature to become unstable limiting the maximal speed of a railway vehicle. Running at sub-critical velocities, the vehicle hunting motion is forced by the random irregularities of the track alignment and it affects the running behaviour and the passengers comfort. The paper deals with the hunting movement of a bogie in the range of the sub-critical velocities in the presence of random irregularities of the alignment. The bogie model has six degrees of freedom and consists of a suspended mass and two wheelsets related to Kelvin-Voigt systems. The wheel/rail friction forces are linear. The elasticity of the track is neglected and only the random irregularities of the alignment are taken into account. First, the critical velocity is calculated and then the frequency-domain response of the bogie is determined for sub-critical velocities. Finally, the acceleration of the bogie due to the irregularities of the track alignment is calculated. The influence of some parameters on the acceleration is pointed out.

1. INTRODUCTION

When a railway vehicle is running along a tangent track, the wheelsets path describes a winding line due to the rolling bi-conic surfaces. This kind of motion is known as the hunting [5, 12].
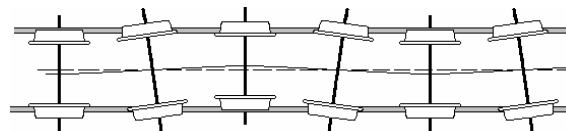
Fig. 1. The wheelset motion.

---

[1] *Assistant Prof. PhD. Stud. Eng., University Politehnica of Bucharest,*
madalinadumitriu@yahoo.com

Figure 1 gives a picture of the hunting of a wheelset. If the wheelset takes a transversally displaced position, the wheel rolling on a larger diameter will advance quicker than the other one, which always stays behind because the wheels are fixed in a rigid manner to the axle's body.

The wheelset spins around the vertical axis and, eventually, will arrive to the track's middle axis. In this moment, the axle spinning angle will be at its highest value and both wheels will roll on even diameters. Next, the wheelset will continue its movement, leaving the centre position to the opposite side in respect to the initial lateral position, forcing the wheel to roll on smaller and smaller diameters and the other one on increasingly larger diameters. Both wheels will reach the same level at the precise moment when the axle centre is situated at the maximum distance from the rail longitudinal axis. From now on, the movement will repeat itself in reverse.

In figure 1, the wheelset motion is only kinematical one because no contact and inertia forces have been into account.

In these circumstances, the wavelength of the wheelset motion is

$$\Lambda = 2\pi \sqrt{\frac{er}{\gamma_e}} \, , \tag{1}$$

where $2e$ is the lateral distance between the two contact points of the wheels, r – the wheel radius and γ_e represents the equivalent conicity of the rolling profiles of the wheels.

This simple formula has been demonstrated by Klingel in 1883 [4] and it shows that the frequency of the wheelset motion increases with the velocity. Indeed, the motion frequency of the wheelset is

$$f = \frac{V}{\Lambda} = \frac{V}{2\pi} \sqrt{\frac{\gamma_e}{er}} \tag{2}$$

and, as it can be seen, the frequency is proportional to velocity.

The wheelsets motion is not a pure rolling motion because the vehicle wheelsets are connected by the bogies or directly by the carbody chassis. In fact, the wheelsets motion is characterized by the so-called creepage representing the slip velocity divided by the forward speed. Corresponding to the creepage, the creepage forces act in the wheels/rails contact patch. In fact, the creepage forces are friction forces. When the creepage values are small, the creepage force increase linear with the creepage. In these circumstances, the equations of motion describing the vehicle hunting are linear.

The dynamics of the railway vehicle represents a balance between the forces acting between the wheel and the rail, the inertia forces and the forces exerted by the suspension and articulation. When the vehicle velocity increases over a particular value – the critical velocity, the vehicle motion becomes unstable [11]. Indeed, the wheelset has the tendency to oscillate at the frequency of the cinematic oscillation. At low

velocities, the frequency is small and the inertia forces are also small. Subsequently, the main component of the resultant force acting on the wheelset is the restoring force due to the elastic connects between the wheelsets and vehicle body. This force will be balanced by the creep force that must be developed. In this way, it results a progressive reduction in lateral displacement as the wheelset pursues its oscillatory path. At high speeds the inertia forces will dominate, as the frequency is correspondingly high. In this case, creep must be developed which will cause a progressive increase in the lateral displacement of the wheelset during its lateral oscillation. It follows that there is a speed at which the successive overshoots neither grow nor decay, the wheelset then, and only then, tracing out a sinusoidal path.

The instability of railway bogie was studied and linear models have been used in many papers [2, 6, 9]. Also, non – linear models were used to study the vehicle/track interaction when the motion becomes unstable [7, 8, 10].

In fact, the range velocity of the railway vehicles must to be a sub-critical one. Indeed, running above the critical speed, the vehicle/track interaction is characterized by very high values of forces acting between wheel and rail and this fact contributes to: the risk of derailment at higher speeds, damage to track, high level of vibration, with bad ride comfort or damage to freight, fatigue failure of the vehicle structure and wear of components.

In this paper, we study the hunting movement from other perspective, considering the range of the sub-critical velocities and the presence of random irregularities of the alignment. This view point is very interesting because it allows describing the dynamic behaviour of the vehicle by means of the acceleration of the bogie.

In this way, we have the possibility to know how the suspension influences the running behaviour and this fact could represent a valuable starting point to improve the design of the bogie.

2. MECHANICAL MODEL

2.1. Equations of motion

The case of a railway vehicle bogie with two wheelsets running uniformly with constant velocity V along a tangent track is considered (fig. 2). The motion is reported to the fixed reference Oxy.

The bogie has a frame of mass m_b and mass moment inertia I_b and two wheelsets of mass m_0 and mass moment inertia I_0.

The suspension has the elastic constants k_x and k_y and the constants damping c_x and c_y. All elastic and damping elements have linear characteristics.

Only the displacements in the horizontal plan are taken into account, respectively, the lateral displacement and the yaw (roll around the vertical axe). The bogie displacements are y_b and α_b and the wheelsets displacements are $y_{1,2}$ and $\alpha_{1,2}$.
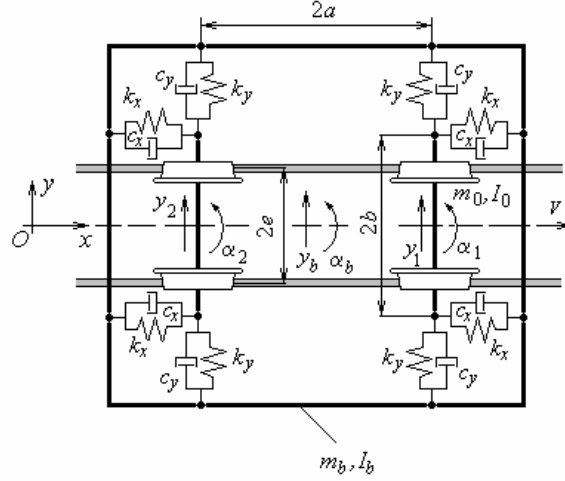
Fig. 2. Mechanical model of the bogie.

Appling the Newton's law, the equations of motion are obtained as follows:
- lateral displacement of the bogie frame

$$m_b \ddot{y}_b + 2c_y(2\dot{y}_b - \dot{y}_1 - \dot{y}_2) + 2k_y(2y_b - \dot{y}_1 - \dot{y}_2) = 0; \qquad (3)$$

- yaw of the bogie frame

$$I_b \ddot{\alpha}_b + 2c_x b^2(2\dot{\alpha}_b - \dot{\alpha}_1 - \dot{\alpha}_2) + 2c_y a(2a\dot{\alpha}_b - \dot{y}_1 + \dot{y}_2) + \\ + 2k_x b^2(2\dot{\alpha}_b - \dot{\alpha}_1 - \dot{\alpha}_2) + 2k_y a(2a\alpha_b - y_1 + y_2) = 0; \qquad (4)$$

- lateral displacement of the first (front) wheelset

$$m_0 \ddot{y}_1 + 2c_y(\dot{y}_1 - \dot{y}_b - a\dot{\alpha}_b) + 2k_y(y_1 - y_b - a\alpha_b) + 2\kappa Q\left(\frac{\dot{y}_1}{V} - \alpha_1\right) = 0; \qquad (5)$$

- yaw of the first (front) wheelset

$$I_0 \ddot{\alpha}_1 + 2\frac{\kappa Q e^2}{V}\dot{\alpha}_1 + 2c_x b^2(\dot{\alpha}_1 - \dot{\alpha}_b) + 2k_x b^2(\alpha_1 - \alpha_b) + 2\kappa Q\frac{e\gamma_e}{r}y_1 = 2\kappa Q\frac{e\gamma_e}{r}\eta_1; \quad (6)$$

-lateral displacement of the second (trailer) wheelset

$$m_0 \ddot{y}_2 + 2c_y(\dot{y}_2 - \dot{y}_b + a\dot{\alpha}_b) + 2k_y(y_2 - y_b + a\alpha_b) + 2\kappa Q\left(\frac{\dot{y}_2}{V} - \alpha_2\right) = 0; \qquad (7)$$

- yaw of the second (trailer) wheelset

$$I_0\ddot{\alpha}_2 + 2\frac{\kappa Qe^2}{V}\dot{\alpha}_2 + 2c_x b^2(\dot{\alpha}_2 - \dot{\alpha}_b) + 2k_x b^2(\alpha_2 - \alpha_b) + 2\kappa Q\frac{e\gamma_e}{r}y_2 = 2\kappa Q\frac{e\gamma_e}{r}\eta_2, \quad (8)$$

where $2a$ is the bogie wheelbase, $2b$ - the distance between the axle boxes, $2Q$ – the static load of the wheelset, κ- the creepage coefficient determined in accordance to Kalker's theory [3].

It has to be underlined that the gyroscopic, restoring gravitational force and spin effects have been neglected according to the opinion of many researches [9, 10, 11].

2.2. Stability

The first issue that has to be solved consists of the stability analysis. As already mentioned, the stability of the vibration of the bogie is related to the so-called critical velocity. This is the velocity at which the bogie becomes unstable. In fact, while running at a velocity lower than the critical value, the vibration of the bogie is stable; on the other hand, when the bogie velocity is higher than the critical one, the vibration of the bogie is not stable any longer – the response of the system to any infinitesimal perturbation intensifies around the steady state position.

To calculate the critical velocity, the roots of the characteristic equation of the motion equations have to be analysed. To this end, the homogenous equations of motion will be considered as follows

$$\mathbf{AX} = 0, \quad (9)$$

where $\mathbf{A}$ is the matrix associated to motion equations and $\mathbf{X}$ is the column vector of generalized displacements

$$\mathbf{X} = \begin{bmatrix} \mathbf{x_b} & \mathbf{x_1} & \mathbf{x_2} \end{bmatrix}^\mathrm{T}, \quad (10)$$

where

$$\mathbf{x_b} = \begin{bmatrix} y_b & \dot{y}_b & \alpha_b & \dot{\alpha}_b \end{bmatrix} \quad (11)$$

$$\mathbf{x_1} = \begin{bmatrix} y_1 & \dot{y}_1 & \alpha_1 & \dot{\alpha}_1 \end{bmatrix} \quad (12)$$

$$\mathbf{x_2} = \begin{bmatrix} y_2 & \dot{y}_2 & \alpha_2 & \dot{\alpha}_2 \end{bmatrix}. \quad (13)$$

To calculate the roots of the characteristic equation is equivalent to calculate the eigenvalues of the $\mathbf{A}$ matrix. This calculation can be performed using the MATLAB function eig.m.

Finally, the eigenvalues of the A matrix, more exactly the real part of these eigenvalues, will indicate whether the system is stable or not.

2.3. Random vibration of the bogie

The second issue refers to the bogie response to random irregularities of the track. We assume that the random irregularities are stationary. In fact, these irregularities are synthetically described by the power spectral density (P.S.D). ORE recommended form can be considered here

$$S(\Omega) = \frac{A\Omega_c^2}{(\Omega^2 + \Omega_r^2)(\Omega^2 + \Omega_c^2)} \, , \tag{14}$$

where Ω is the wave number, $\Omega_c = 0,8246$ rad/m, $\Omega_r = 0,0206$ rad/m, and $A = 2,119 \cdot 10^{-7}$ rad m or $A = 6.125 \cdot 10^{-7}$ rad m, depending on the track quality.

The track irregularities are the excitation factor for the bogie running at the speed V along the track and this is why the P.S.D. irregularities need to be expressed as a function of the angular frequency $\omega = V\Omega$

$$G(\omega) = \frac{A\Omega_c^2 V^3}{[\omega^2 + (V\Omega_c)^2][\omega^2 + (V\Omega_r)^2]} \, . \tag{15}$$

Stating from the bogie frequency-domain response described by the column vector

$$\overline{\mathbf{H}}(\omega) = \begin{bmatrix} \overline{H}_b^y & \overline{H}_b^\alpha & \overline{H}_1^y & \overline{H}_1^\alpha & \overline{H}_2^y & \overline{H}_2^\alpha \end{bmatrix}^\mathrm{T} \tag{16}$$

and the track irregularities P.S.D., the column vector of the acceleration P.S.D. can be calculated

$$\mathbf{G_b}(\omega) = \omega^4 G(\omega) \left| \overline{\mathbf{H}}(\omega) \right|^2 \, , \tag{17}$$

and then, the column vecotor of the r.m.s. acceleration

$$\mathbf{a_b} = \sqrt{\frac{1}{\pi} \int_0^\infty \mathbf{G_b}(\omega) d\omega} \, . \tag{18}$$

In fact, we are interested only by the range frequency of 0 – 20 Hz, and the limit of integration is removed corresponding to the particular value of frequency. The frequency response can be calculated considering the harmonic steady state behaviour. To this end, the displacements and the excitation have the following form

$$\overline{y}_b = \overline{Y}_b e^{i\omega t} \, , \ \overline{\alpha}_b = \overline{A}_b e^{i\omega t} \, , \ \overline{y}_1 = \overline{Y}_1 e^{i\omega t} \, , \ \overline{\alpha}_1 = \overline{A}_1 e^{i\omega t}$$

$$\overline{y}_2 = \overline{Y}_2 e^{i\omega t} \, , \ \overline{\alpha}_2 = \overline{A}_2 e^{i\omega t} \, , \ \overline{\eta}_{1,2} = \overline{\eta}_0 e^{\pm i\frac{\omega a}{V}} e^{i\omega t} \tag{19}$$

where $\bar{Y}_b$, $\bar{A}_b$, …, $\bar{\eta}_0$ are complex amplitudes, and ω is the angular frequency.

The equations of motion can be written as

$$(-\omega^2 \mathbf{M} + i\omega \mathbf{C} + \mathbf{K})\bar{\mathbf{q}} = \bar{\mathbf{F}}, \tag{20}$$

where $\mathbf{M}$, $\mathbf{C}$ and $\mathbf{K}$ are the mass, viscous damping and stiffness matrices. The column vectors $\bar{\mathbf{q}}$ and $\bar{\mathbf{F}}$ are defined as follows

$$\bar{\mathbf{q}} = \begin{bmatrix} \bar{y}_b & \bar{\alpha}_b & \bar{y}_1 & \bar{\alpha}_1 & \bar{y}_2 & \bar{\alpha}_2 \end{bmatrix}^{\mathrm{T}} \tag{21}$$

$$\bar{\mathbf{F}} = 2\kappa \frac{e}{r} \gamma_e Q \bar{\eta}_0 \begin{bmatrix} 0 & 0 & 0 & e^{i\frac{\omega a}{V}} & 0 & e^{-i\frac{\omega a}{V}} \end{bmatrix}^{\mathrm{T}}. \tag{22}$$

Solution of the equation (20) can be obtained

$$\bar{\mathbf{q}} = (-\omega^2 \mathbf{M} + i\omega \mathbf{C} + \mathbf{K})^{-1} \bar{\mathbf{F}}. \tag{23}$$

Finally, the frequency-domain response of the bogie can be calculated

$$\bar{\mathbf{H}} = \frac{\bar{\mathbf{q}}}{\bar{\eta}_0}. \tag{24}$$

Now, introducing the frequency-domain response of the bogie in equations (17) and (18), we can calculate the r.m.s. acceleration, obtaining an interesting description of the bogie running behaviour.

3. NUMERICAL APPLICATION

This chapter showcases the results of a numerical application done for Y32 bogie that travels at different velocities on a tangent track with random irregularity. The track irregularity PSD from equation (14) is taken into account.

The parameters of the bogie model are as such: m_b= 3700 kg, I_b = 3800 kgm^2, m_0= 1400 kg, I_0 = 790 kgm^2, k_x = 50 MN/m, k_y = 7 MN/m, c_x = 30 kNs/m, c_y = 11 kNs/m, $2e$ = 1.5 m, $2a$ = 2.56 m, $2b$ = 2 m, r = 0.445 m, γ_e = 0.124, κ = 188, $2Q$ = 110 kN. The equivalent conicity value corresponds to the CFR S 78 wheel profile and UIC 60 rail.

First, we calculate the critical velocity following the method presented in the section 2.2. The critical velocity of the Y 32 bogie has the value of 259.45 km/h (72.07 m/s), of 30 % higher than the operational maximum velocity (200 km/h).

Figure 3 displays the critical velocity versus the longitudinal stiffness for three values of the lateral stiffness. In general, the critical velocity depends strongly by both longitudinal and lateral stiffness.
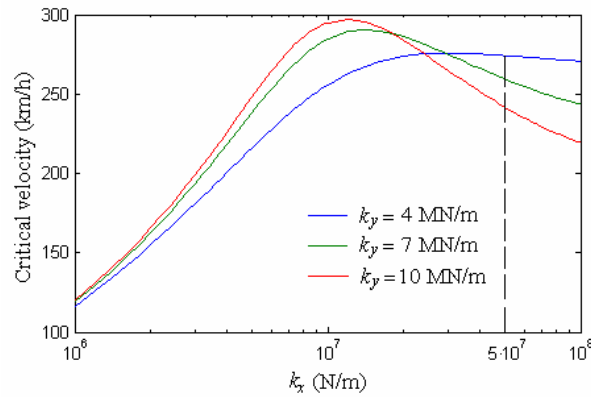
Fig. 3. Influence of k_x on the critical velocity.

The critical velocity increases as long as the longitudinal stiffness increases but remains lower then 10 MN/m for all three values of the lateral stiffness. The critical velocity has a maximum value depending on the lateral stiffness. Any way, choosing primary suspensions parameters is a difficult problem because there are many criteria and the critical speed is only one of them. However, for the reference value of the longitudinal stiffness, the influence of the lateral stiffness on the critical velocity is relatively less evident. This fact is relevant because the stiffness of the suspension changes during the operational service.
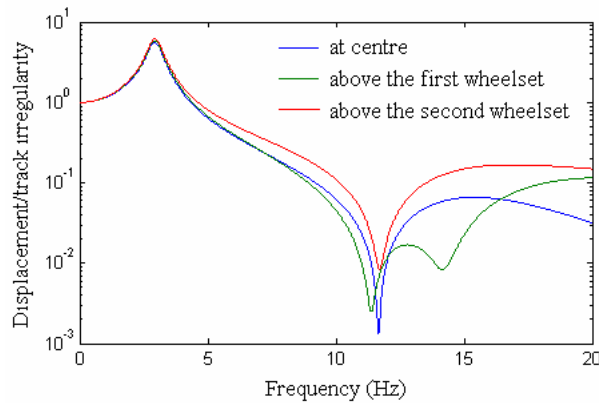
Fig. 4. Frequency-domain response of the bogie.

Next, the sub-critical velocities range is examined. Figure 4 shows the frequency-domain response of the bogie at 200 km/h. The lateral displacement of the bogie at centre and above the two wheelsets is presented. The response is dominated by the frequency of 2.94 Hz.

On the other hand, the bogie response exhibits a anti-resonance frequency

around 11 Hz due to the geometric filter effect. Indeed, the size of irregularities against each axle depends on its position. Thus, bearing reference to the track irregularity against the bogie centre, the defects against the wheelsets are dephased with $\pm 2\pi a/\Lambda$. Against each wheelset, the irregularity is dephased corresponding to the bogie axle base and to the velocity V of traveling over the irregularities of track – all these will trigger an imposed movement for the bogie that becomes time function

$$\eta_{1,2} = \eta_0 \cos\frac{\omega}{V}(Vt \pm a) ,\qquad (25)$$

where $\omega = 2\pi V/\Lambda$ is the angular frequency.

The excitation caused by the track irregularities introduces the factor $\cos\omega a/V$ which multiplies the frequency-domain response of the bogie. This excitation mode will bring a series of maximum and minimum values that are conditional upon the velocity.

For instance, for the frequencies $f_n = (2n+1)V/4a$ with $n = 0, 1, 2, \dots$, the bogie response is minimum due to the geometric filtering effect. For $n = 0$ and $V = 55, 56$ m/s (200 km/h), we have

$$f_0 = V/4a = 10.85 \text{ Hz}.$$

Similar effect has been reported for the vertical vibration of the railway vehicles [1].
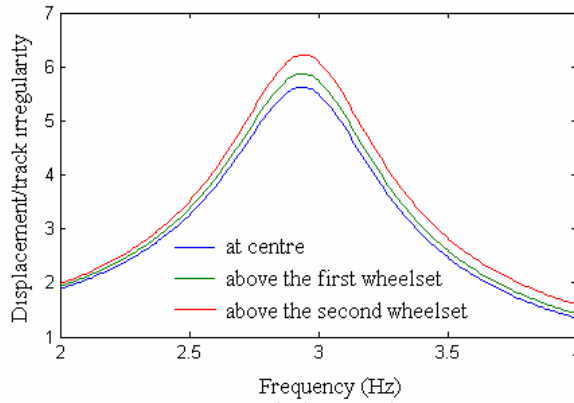
Fig. 5. Frequency-domain response of the bogie (2-4 Hz).

Figure 5 represents the frequency-domain response for frequencies between 2 and 4 Hz to point out that the minimum response is signaled at the bogie centre. Also, the response above the second wheelset is higher than one above the first wheelset.

The influence of the velocity on the running behaviour of the bogie is presented in figure 6, where the acceleration of the bogie is displayed. In fact, the bogie acceleration at the centre and above the two wheelset is calculated using equation (18)

to obtain the r.m.s. value for velocities between 50 and 250 km/h. The acceleration increases continually little by little up to the velocity of 200 km/h. When the velocity passes over this value, the acceleration grows up very strong because the bogie has the tendency to lose its stability. The results are consistent with the ones derived from previous figure and the acceleration above the second wheelset is highest. Then, the acceleration above the first wheelset follows.
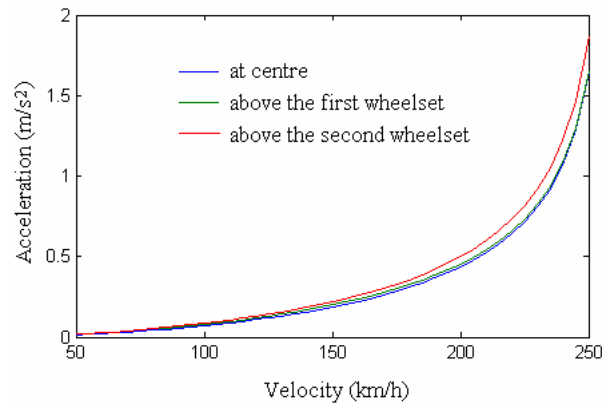
Fig. 6. Bogie acceleration versus velocity.

Figures 7, 8 and 9 display the bogie acceleration versus the longitudinal stiffness k_x, when the bogie is running at 200 km/h. For the lateral stiffness has been taken into account three values, 4, 7 and 10 MN/m. The bogie acceleration is calculated at the centre and above the two wheelsets.

It can be observed that the bogie acceleration in all three points has the same feature depending on the longitudinal stiffness. The acceleration takes the highest value above the second wheelset and the lowest ones at the centre.
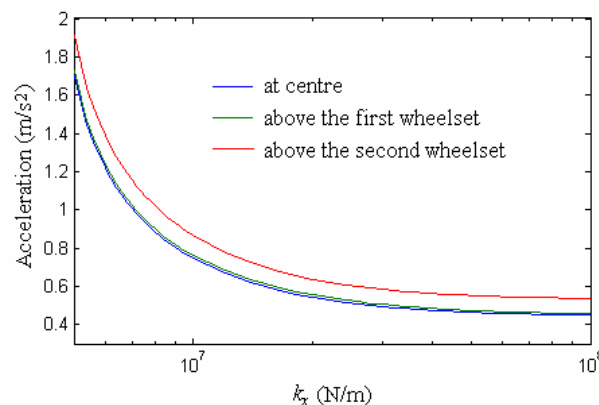
Fig. 7. Bogie acceleration versus longitudinal stiffness at 200 km/h (k_y = 4 MN/m).
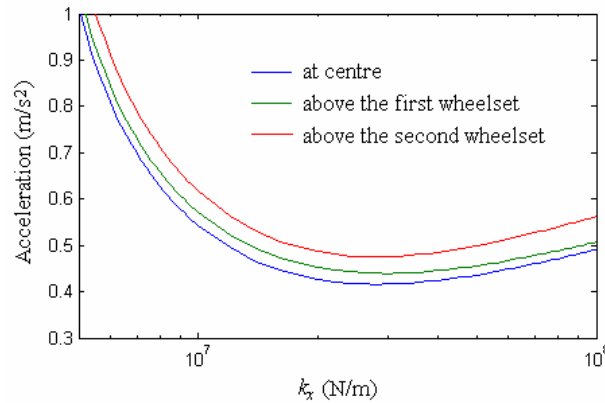
Fig. 8. Bogie acceleration versus longitudinal stiffness at 200 km/h (k_y = 7 MN/m).
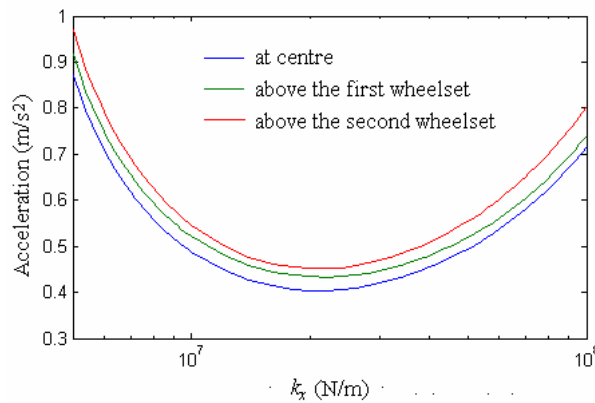
Fig. 9. Bogie acceleration versus longitudinal stiffness at 200 km/h (k_y = 10 MN/m).

The stiffness influence on the bogie acceleration depends very much on the lateral stiffness. When the value of 4 MN/m is considered for the lateral stiffness, the bogie acceleration decreases as long as the longitudinal stiffness value increases (see. Fig. 7). However, increasing the longitudinal stiffness beyond the value of 2 MN/m, the bogie acceleration remains practically constant.

Different story can be seen in figures 8 and 9, where it seems that we have particular value of k_x that correspond to the minimum acceleration.

Figures 10, 11 and 12 show the influence of the longitudinal stiffness on the bogie acceleration above the second wheelset at three velocities, 100, 150 and 200 km/h taking in consideration the same values of the lateral stiffness, 4, 7 and 10 MN/m. When the speed decreases, the influence of the longitudinal stiffness on the bogie acceleration became imperceptible for a large range between 10 and 100 MN/m. This aspect seems to be independent on the value of the lateral stiffness.
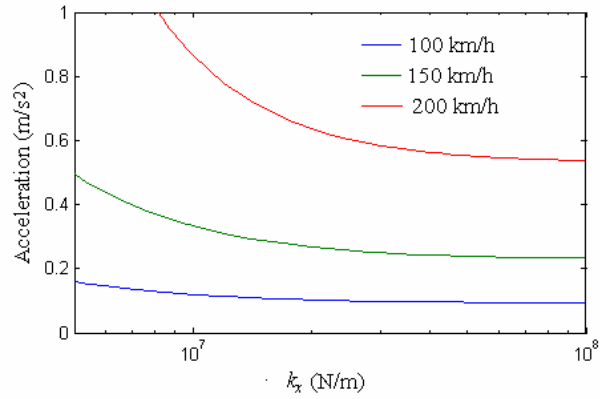
Fig. 10. Bogie acceleration above the second wheelset versus longitudinal stiffness for different speeds and $k_y = 4$ MN/m.
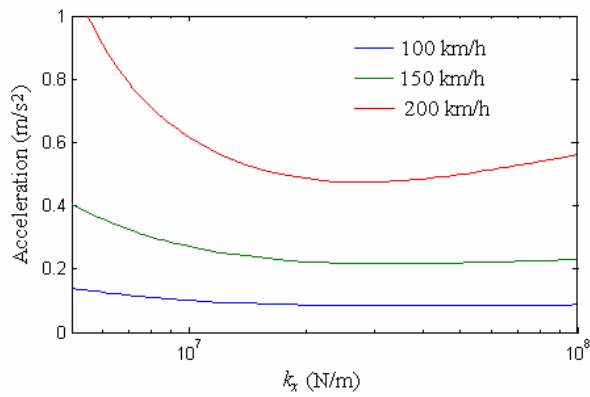
Fig. 11. Bogie acceleration above the second wheelset versus longitudinal stiffness for different speeds and $k_y = 7$ MN/m.
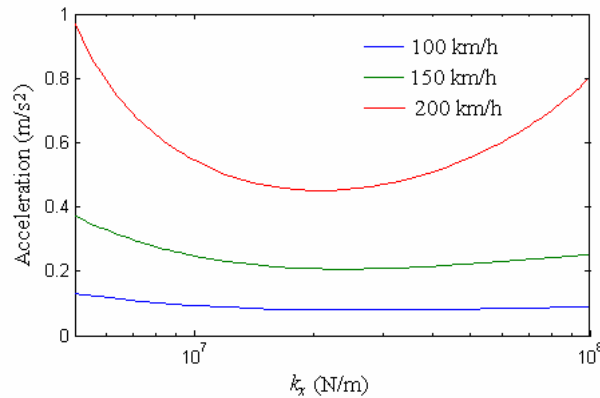
Fig. 12. Bogie acceleration above the second wheelset versus longitudinal stiffness for different speeds and $k_y = 10$ MN/m.

4. CONCLUSIONS

In this paper, the hunting movement of a bogie in the range of the sub-critical velocities in the presence of random irregularities of the alignment is studied in order to point out the influence of the suspension stiffness on the running behaviour. For this task, the six degree of freedom bogie model including the suspended mass and two wheelsets related to Kelvin-Voigt systems is considered. The wheel/rail friction forces are linear. The elasticity of the track is neglected and only the random irregularities of the alignment are taken into account.

When the bogie speed is high, relatively close to critical value, the influence of the suspension stiffness on the bogie acceleration is important and we can speak about the best value of the stiffness. However, at relative low velocities, the influence of the suspension stiffness is less obvious.

REFERENCES

[1]. **Dumitriu, M.,** *Geometric filtering effect of vertical vibrations in railway vehicles*, Analele Universității "Eftimie Murgu" Reşiţa, Anul XIX, nr. 1, pp. 48-61, 2012.
[2]. **Joly, R.,** *Étude de la stabilité transversale d'un véhicule ferroviaire circulant à grande vitesse*. ORE DT 16/F Utrecht, octobre 1970.
[3]. **Kalker, J.J.,** *On the Rolling Contact of Two Elastic Bodies in the Presence of Dry Friction. Dissertation*, TU Delft, 1967.
[4]. **Klingel, W.,** *Über den Lauf der Eisenbahnwagen auf gerader Bahn*, Organ für die Fortschritte des Eisenbahnwesens, 20, 113-123, Table XXI, 1883.
[5]. **Knothe, K., Böhm, F.,** *History of Stability of Railway and Road Vehicles*, Vehicle Systems Dynamics 31, pp. 393-421, 1999.
[6]. **Lee, S.Y., Cheng, Y.C.,** *Hunting stability analysis of high-speed railway vehicle trucks on tangent tracks*, Journal of Sound and Vibration 282, pp. 881-898, 2005.
[7]. **Mazilu, T.,** *An analysis of bogie hunting instability*, U.P.B. Scientific Bulletin, Series D, Vol. 71, Iss. 2, 2009.
[8]. **Pascal, J.P.,** *Calcul dynamic par VOCO des forces du contact roue/rail validation par les essais en lighe d'un wagon à essieux testé par la SNCF entre Hirson et Charleville*, Rapport INRETS no 169, 1993.
[9]. **Sebeşan, I., Mazilu, T.,** *Vibraţiile vehiculelor feroviare*, (Vibrations of the railway vehicles), Editura Matrix Rom, Bucureşti, 2010.
[10]. **True, H.,** *On the Theory of Nonlinear Dynamics and its Applications in Vehicle Systems Dynamics*, Vehicle Systems Dynamics 31, 393-421, 1999.
[11]. **Wickens, A.H.,** *Fundamentals of rail vehicles dynamics Guidance and Stability*, Swets & Zeitlinger, 2003.
[12]. **Wickens, A.H.,** *The dynamics of railway vehicles-from Stephenson to Carter*. Proceedings of the Institution of Mechanical Engineers, Part F: Journal of Rail and Rapid Transit, 212, 209-217, 1998.